Stabilization of Urate Oxidase Using Deep Eutectic Solvents Comprising Sucrose, Fructose, and Glycerol via Molecular Dynamics Simulation

Zahra Soltani-Nezhad[1],* Maryam Zaboli[2], Mojtaba Mortazavi[1], Masoud Torkzadeh-Mahani[1]
[1] Department of Biotechnology, Institute of Science, High Technology and Environmental Sciences, Graduate University of Advanced Technology, Kerman, Iran, Zahra.sn1729@gmail.com, mtmahani@gmail.com
[2] Department of Chemistry, Faculty of Science, University of Birjand, Birjand, Iran

ABSTRACT

Serum uric acid levels are commonly assessed in human and other mammalian studies. Given the evolutionary loss of the gene encoding uricase in these species, elevated uric acid levels may lead to conditions such as tumor lysis syndrome, gout, and renal disorders. Consequently, the stability of this enzyme has garnered significant interest among researchers. Among various stabilization methods, the utilization of natural deep eutectic solvents (DESs) has been favored due to their numerous advantages over alternative approaches. In this study, DES was synthesized using three components: fructose, sucrose, and glycerol. Recombinant uricase (rasburicase) was produced in the BL21 bacterial strain, followed by protein purification using a nickel-affinity column. The optimal solvent concentration for the corresponding enzyme was determined, and molecular dynamics simulations were performed at this optimal concentration over a duration of 35 nanoseconds using GROMACS software. Analyses of RMSD, RMSF, SASA, and R_g were conducted, revealing reductions in these values, which correlate with decreased structural fluctuations and enhanced structural compactness. Additionally, analyses of RDF, total energy (sum of electrostatic and Lennard-Jones interactions), and number of contacts for each eutectic component were calculated, with sucrose exhibiting the highest values relative to the other components. Overall, molecular dynamics simulation results indicated an increase in enzyme stability in the presence of the eutectic compared to the free enzyme.

Keywords: *Uricase, Deep Eutectic Solvent, Molecular Dynamics Simulation, Optimal Concentration.*

1. *INTRODUCTION*

*Uricase (urate oxidase) is a non-glycosylated [1] homotetramer [2] (***Fig 1***) belonging to the oxidoreductase family, comprising four identical subunits, each weighing 30 kilodaltons [3]. This enzyme is present across all three domains of life [4]; however, during evolutionary processes, it has been lost from the genomes of mammals, certain reptiles, and birds [5]. Rasburicase, a recombinant form of uricase [6], has a molecular mass of 135 kilodaltons and consists of 302 amino acids [3, 7]. The active site of uricase is located on the external surface of the tetramer, at the interface between subunits A-B and C-D (between S7 and S8), and is composed of key amino acids including lysine 10 (which forms hydrogen bonds with threonine 57 and histidine 256), threonine 57, phenylalanine 159, arginine 176, glutamine 228, and asparagine 254. Proline 284 and glycine 286, positioned between lysine 10 and asparagine 254, likely play a crucial structural role in maintaining the conformation of the enzyme's active site. Additionally, leucine 170 and phenylalanine 159 create a hydrophobic pocket for the enzyme's substrate [8]. Uric acid ($C_5H_4N_4O_3$) acts as the substrate for uricase, being a heterocyclic molecule with a molecular weight of 168.11 Da [9] and representing the final product of purine catabolism [10-12]. Prolonged elevation of uric acid levels in the body is associated with various complications, including tumor lysis syndrome, hyperuricemia, gout, and renal failure [13]. In many birds and primates, including humans and chimpanzees, the uricase gene has become inactive during evolution, leading to the accumulation of uric acid as the terminal product of purine metabolism [14]. Nevertheless, the administration of rasburicase has been shown to reduce uric acid levels [6]. Given the*

significance of uricase, particularly in therapeutic contexts, numerous researchers have sought to explore methodologies for enhancing the stability of this enzyme. One such approach involves the use of additives as stabilizing agents [15, 16]. Natural deep eutectic solvents [17], composed of substances like amino acids and sugars, have garnered attention due to their numerous advantages, including low toxicity, cost-effectiveness, and high solubility, contributing to enhanced enzyme stability [15]. Generally, deep eutectic solvents (DES) are obtained by heating or mixing donor and acceptor hydrogen-bonding groups in a specific ratio [18].

Typically, to predict enzyme properties and investigate the impact of various phenomena, researchers employ two methodologies: experimental laboratory tests and computer-based simulations. While experimental procedures often require substantial costs and time, the latter approach, which relies on simulations, alleviates these constraints and provides valuable insights into structural changes in proteins. Molecular dynamics (MD) simulation is one of the most important computational tools for studying protein structures [19], enabling theorists to model and predict outcomes based on their theoretical frameworks [20, 21]. In simulations, after reviewing the substance of interest, an initial model is constructed, and the positions and velocities of atoms are determined using appropriate software [22-24]. Subsequently, suitable interactions between two molecules are selected, and new velocities are computed based on intermolecular forces. Finally, interaction energies are assessed to confirm equilibrium within the system [25]. This methodology has been applied across various chemical, biochemical, materials science, and polymer systems, representing a novel advancement in the field of bioinformatics. Utilizing this technique also allows for the investigation of the structures of biomacromolecules, analysis of structural complexes, and examination of their structural interactions, paving the way for potential modifications

In this study, we investigate the effects of a DES composed of sucrose, fructose, and glycerol on the stability of uricase through molecular dynamics simulations.

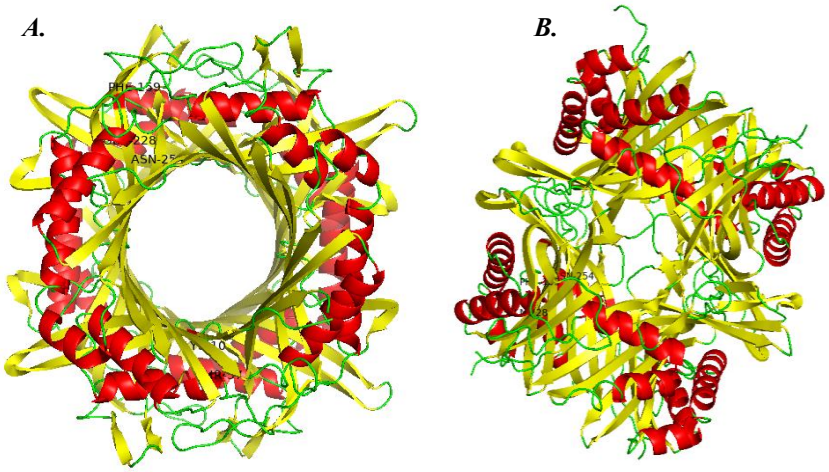

Fig 1. *Molecular structure of the uricase tetramer, depicted using PyMOL. A. Lateral view; B. Frontal view.*

2. *MATERIALS AND METHODS*

2.1 Materials

The following reagents were utilized in this study: tryptone, yeast extract, agar, sodium chloride (NaCl), potassium hydrogen phosphate (K_2HPO_4), potassium dihydrogen phosphate (KH_2PO_4), IPTG, sodium hydrogen phosphate (NaH_2PO_4), imidazole, uric acid, ammonium persulfate (APS), tetra methyl ethylene diamine (TEMED), Tris-HCl, tetraborate, acetic acid, methanol, glycine, EDTA, nickel sulfate ($NiSO_4$), and phosphoric acid.

Escherichia coli BL21 containing the recombinant plasmid pET28a$^+$_UOX was employed as the bacterial strain, while kanamycin served as the antibiotic. Protein purification was conducted using NI-NTA nickel affinity chromatography. Fructose, sucrose, and glycerol were utilized for the synthesis of the deep eutectic solvent (DES). Luria-Bertani medium was prepared for bacterial culture.

2.2 Bacterial Culture and Protein Production

The BL21 bacterial strain harboring the recombinant plasmid pET28a^{+}_UOX was cultured in sterile Luria-Bertani medium supplemented with agar (comprising 1 g tryptone, 0.5 g yeast extract, 1 g NaCl, and 1.5 g agar in 0.1 L deionized water) and kanamycin. The culture was incubated at 37°C for 13 to 14 hours. Subsequently, a suitable colony was transferred to 10 mL of liquid LB medium (prepared with the same ratio but without agar) containing the antibiotic and incubated overnight at 37°C for 16 to 17 hours. 1 mL of this overnight culture was then added to 100 mL of TB medium (containing 90 mL of base components, which included 1.2 g tryptone, 2.4 g yeast extract, and 0.4 mL glycerol, along with 10 mL of salts comprising 1.2 g K_2HPO_4 and 0.23 g KH_2PO_4). Upon reaching the desired optical density (OD) of 0.5, protein expression was induced by adding 2 mL of 1 M IPTG for 5 hours. The resulting solution was subjected to sonication and centrifugation at 13,000 rpm for 20 minutes at 4°C to facilitate the purification process, after which it was transferred to the nickel affinity column. Protein expression was assessed via SDS-PAGE electrophoresis.

2.3 Synthesis and Optimization of DES Concentration

*For the synthesis of DES, the required amounts of sucrose (**Fig 2-A**), fructose (**Fig 2-B**), and glycerol (**Fig 2-C**) were weighed and mixed under heating (**Table 1**). The resulting clear solution was stirred for an additional 15 minutes to achieve a semi-solid and viscous environment.*

*Subsequently, to determine the optimal concentration of the eutectic, seven different concentrations were prepared in the presence of Tris-HCl buffer (pH = 8.5), and the absorbance spectrum was recorded using a spectrophotometer over the wavelength range of 200 to 700 nanometers. This procedure was also performed for the burax buffer containing the substrate, and a concentration below 10% was selected. The enzymatic activity was measured using the formula (**1**) for concentrations of 1%, 5%, and 10% for the eutectic enzyme, with the free enzyme diluted in Tris serving as the control.*

Table 1. DES Synthesis

Materials	Amount
Sucrose	2 mMol
Fructose	2 mMol
Glycerol	4 mMol
Distilled water	1 mMol

$$Volume\ activity\ \left(\frac{u}{ml}\right) = \frac{\Delta(A_0 - A_{60}).V.D}{12{,}6.d.v} \qquad \textbf{(1)}$$

A_0 is the absorbance without substrate, A_{60} is the absorbance in the initial minute, V is the total reaction mixture volume (0.730 mL), D represents enzyme extinction coefficient, 12.6 is the molar absorptivity of uric acid ($mM^{-1}.cm^{-1}$), d is the path length (1 cm), and v refers to the enzyme sample volume (0.02 mL).

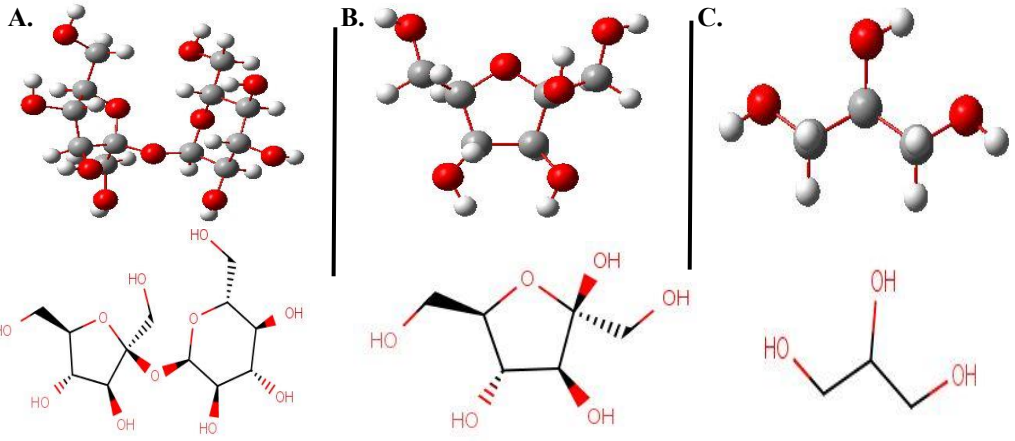

Fig 2. *Drawing two and three-dimensional structure of eutectic components. **A.** Sucrose, **B.** Fructose and **C.** Glycerol.*

2.4 Molecular Dynamics Simulation

Molecular Dynamics (MD) simulation provides a molecular perspective on the interactions between the molecules present in the eutectic and the enzyme under investigation [26]. For this purpose, the initial structure of uricase, with the code 1R56, was utilized from the protein database [λ]. Molecular simulations were conducted using GROMACS version 2023 and the CHARMM27 force field [27]. To maintain the temperature at an optimal 35°C, the Velocity Rescaling algorithm was employed [28]. *Furthermore, the Berendsen algorithm was applied to regulate pressure at 1 bar. The Particle-Mesh Ewald (PME) method was used for estimating long-range electrostatic interactions [29], and the Lennard-Jones potential described van der Waals interactions at a cutoff distance of 1.4 nm to limit non-covalent interactions [30]. The LINCS algorithm was implemented to impose constraints on all covalent bonds* [31], *while the Grid algorithm facilitated the search for neighboring cells. The Steepest Descent (SD) algorithm was utilized for energy optimization under constant pressure and temperature, ensuring system equilibrium and preventing inappropriate geometric and spatial overlaps. Ultimately, the final stages of the simulation were conducted for 35 ns.*

*Root Mean Square Deviation (RMSD) analysis (**2**) was performed on the alpha carbon atoms to compare the protein structure before, during, and after the simulation, examining the conformational changes in the enzyme in the presence and absence of the eutectic [32]. Subsequently, Root Mean Square Fluctuation (RMSF) analysis (**3**) was conducted to assess the flexibility of the protein and its structural variations, focusing on the residues that exhibit the highest accessibility within different structural regions [33]. The Solvent Accessible Surface Area (SASA) reflects the solvent's accessibility to the amino acids within the protein structure, thereby providing insights into the stability of the protein chain [34]. Another critical parameter in studying structural changes and protein compactness during the reaction is the Radius of Gyration (**4**), which indicates the distribution of components along the principal axis. For each molecule, the distance from the center of mass was calculated, followed by squaring these distances. The mean square of these distances was then computed, with its square root representing the Radius of Gyration [35].*

$$RMSD = \sqrt{\frac{1}{N}\sum_{i=1}^{N}\left(r_i(t) - r_i(0)\right)^2} \quad \textbf{(2)}$$

$$RMSF = \sqrt{\frac{1}{T}\sum_{i=1}^{T}(r_i(t) - \langle r_i \rangle)^2} \quad \textbf{(3)}$$

$$R_g = \sqrt{\frac{1}{N}\sum_{i=1}^{N}(r_i - r_{cm})^2} \quad . r_{cm} = \frac{1}{M}\sum_{i=1}^{M} r_i m_i \quad \textbf{(4)}$$

In these equations, RMSD represents the root mean square deviation (nm), RMSF denotes the root mean square fluctuation (nm), R_g indicates the radius of gyration (nm), N refers to the number of atoms or particles, $r_i(t)$ is the position of atom i at time t, T signifies the number of simulation frames, $\langle r_i \rangle$ is the average position of atom i throughout the simulation, r_{cm} denotes the center of mass position of the molecule, M is the total mass, and m_i represents the mass of atom i.

*Subsequently, each component of the eutectic was examined individually. The radial distribution function (RDF) analysis (**5**) was performed to determine the probability density of a particle's presence at a specified distance from the enzyme or other particles throughout the simulation, as well as to assess the interaction strength for each eutectic component separately. Van der Waals interaction energies were calculated using the Lennard-Jones potential, while electrostatic interactions were computed employing the Long-range algorithm. The cumulative graph of these two energy types was plotted against time. To assess the number of molecular collisions with the enzyme over time, the collision radius between particles was first defined, and the distance between particle pairs was determined. A collision was registered if the distance between two*

particles was less than the defined collision radius. Thus, the number of collisions was directly calculated by counting the frequency at which particles approached one another.

$$g(r) = \frac{V}{N^2}, \frac{dN}{dr} \quad \textbf{(5)}$$

g(r) is defined as the radial distribution function (nm), V represents the total volume of the system, N is the number of particles, and r is the radius of the spherical shell (nm).

3. *RESULTS AND DISSCUTION*

3.1 Bacterial Culture and Protein Purification

*The cultivation of BL21 bacteria containing the recombinant uricase plasmid was conducted in a medium supplemented with kanamycin. Single colonies were utilized for further culturing (***Fig *3***). The pET28a$^+$ plasmid serves as a high-copy expression vector [36, 37], comprising the T7 promoter, the lac repressor, and a His-tag, which are appended to both the N- and C-termini of the protein. Additionally, it contains a gene conferring resistance to kanamycin, which is employed during the screening process. The BL21 strain possesses the laci gene, which encodes the lacUV5 repressor, inhibiting expression under normal conditions, alongside the DE3 genetic segment that harbors the lacUV5 promoter and the T7 RNA polymerase gene [38]. In the presence of IPTG, the inhibition of laci and subsequent cessation of its activity activates the lacUV5 promoter, leading to the transcription of the T7 RNA polymerase-encoding gene. E. coli is a Gram-negative bacterium with an optimal growth temperature of 37 °C [39]. Excessive expression, resulting from prolonged induction time, increased inducer concentration, or temperatures exceeding the optimal range, can lead to reduced yield due to bacterial cell death. In this study, based on prior research, an induction period of 5 hours and an IPTG concentration of 1 M at 37 °C were established.*

Uricase contains a histidine tag, which exhibits a strong affinity for nickel ions. The purification of the produced enzyme was achieved through nickel affinity chromatography, followed by competitive elution using imidazole to separate the enzyme from the column. Imidazole, having a higher affinity for nickel ions, displaces the enzyme, facilitating its elution from the column.

Fig 3. *The bacterial culture containing the plasmid was maintained in a kanamycin-supplemented growth medium, from which single colonies were selected for subsequent procedures.*

3.2 Eutectic Synthesis and Optimal Concentration Determination

In the synthesis of DES from glycerol, fructose, and sucrose, glycerol was highlighted for its critical role. Pajang et al. noted that glycerol, by distancing itself from proteins and interacting with hydrophobic surface sites, prevents the inactive aggregation of protein structures, thereby enhancing their stability [40]. This viscous, non-volatile, non-toxic, and biodegradable substance boasts a high boiling point. Additionally, Lin et al. reported that sucrose increases surface tension, leading to protein hydration and consequently improving protein stability [41].

*Subsequently, the optimization of eutectic concentration was performed, selecting a range of 1% to 10%. Concentrations exceeding 10% exhibited higher absorption spectra than uric acid, resulting in spectral interference that disrupted enzyme adsorption and activity assessment (***Fig 4***). Following activity measurements, a 5% eutectic concentration was determined to be optimal within the total enzyme volume (***Fig 5***).*

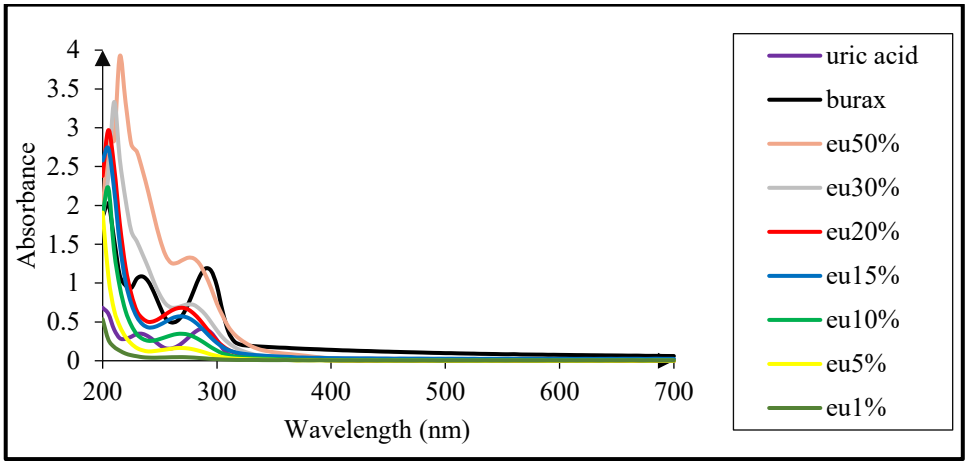

Fig 4. *A comparative analysis of the absorbance intensities of various eutectic concentrations across wavelengths from 200 to 700 nanometers alongside the absorbance intensity of burax containing uric acid within the same wavelength range.*

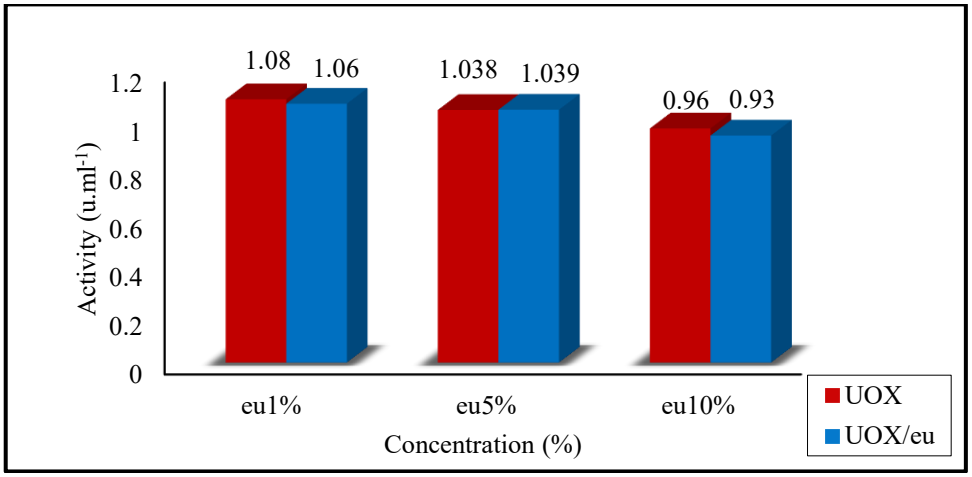

Fig 5. *Comparison of the activity of free enzyme (red) versus enzyme containing eutectic (blue) at a wavelength of 293 nanometers to ascertain the optimal concentration.*

3.3 Molecular Dynamics

*The Root Mean Square Deviation (RMSD) analysis serves as a critical metric for assessing the influence of solvent on the stability and structural integrity of proteins over time (***Fig 6***). The results indicate that, during the initial stages of the simulation, the RMSD profiles in both the presence and absence of the eutectic solvent are nearly superimposed. However, over time, a notable decrease in RMSD values is observed in the presence of the eutectic, which may be attributed to constraints on the structural freedom of the enzyme, ultimately leading to enhanced stability. A study conducted by Zabali et al. corroborates this observation, demonstrating that the fluctuations of the treated enzyme are significantly reduced compared to those of the free enzyme, suggesting a decrease in variability and an increase in stability over time [42].*

*In terms of Root Mean Square Fluctuation (RMSF) analysis, the highest fluctuations were observed in the terminal residues of the protein structure (**Fig 7**), likely due to the greater flexibility of these residues compared to those in the central region. Furthermore, in the presence of the eutectic solvent, these fluctuations are diminished relative to the free enzyme, indicating enhanced stability of the residues and a reduction in their mobility and interaction. Residues characterized by lower mobility and greater structural stability often represent critical regions that play vital roles in various biological processes.*

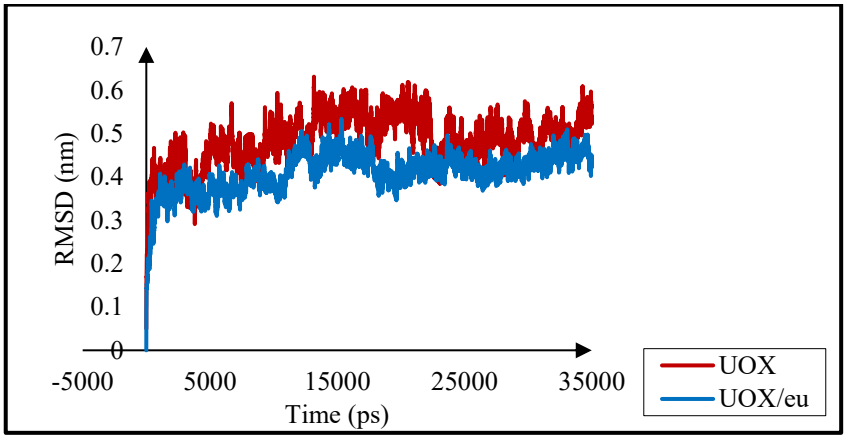

Fig 6. *RMSD Analysis in the presence (blue) and absence (red) of the eutectic solvent over the simulation duration (35 ns).*

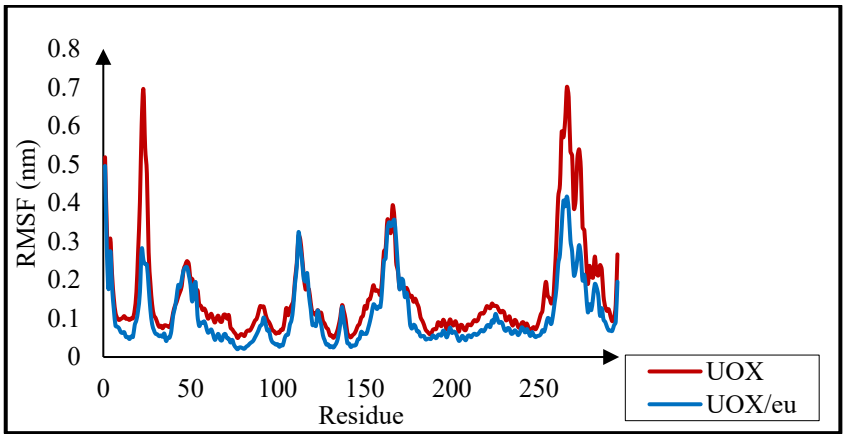

***Fig 7**. RMSF Analysis concerning structural fluctuations of the enzyme in both the presence (blue) and absence (red) of the eutectic.*

*The Solvent Accessible Surface Area (SASA) throughout the simulation remains relatively stable in both conditions, with lower values observed in the presence of the eutectic solvent compared to the free state (**Fig 8**). This reduction in SASA suggests that a smaller surface area is accessible to the solvent, which is commonly associated with more stable structures or situations in which the molecule is aggregating. A study by Khajesteband et al. further supports this notion, indicating that a decrease in SASA correlates with an increase in intramolecular hydrogen bonding, enhanced structural compactness, reduced solvent accessibility, and improved thermodynamic stability [43].*

*The changes in the Radius of Gyration (Rg) at the onset of the analysis are nearly identical in both scenarios, with an increase in simulation time to 35 nanoseconds resulting in a decrease in Rg in the presence of the eutectic compared to the free enzyme (**Fig 9**). This reduction signifies an increase in the density and complexity of the protein structure. The similarity of Rg values for both the free enzyme and the eutectic-treated enzyme at the beginning and end of the simulation confirms the dynamic stability of the protein.*

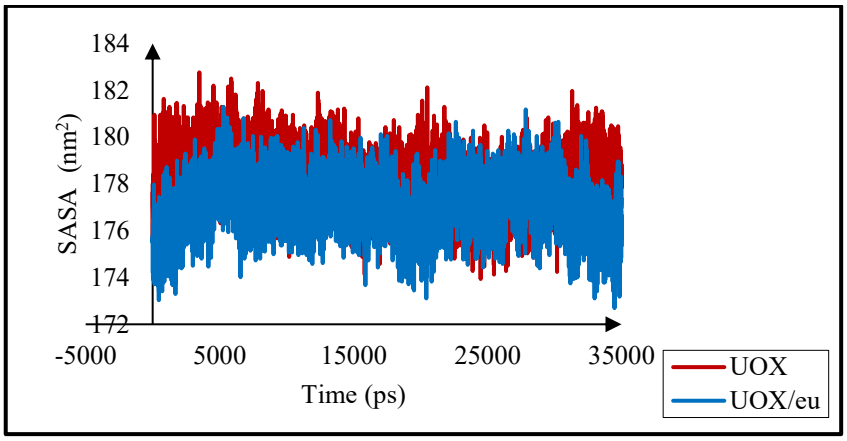

Fig 8. *SASA Values and calculations of solvent-accessible surface area for both the free enzyme (red) and the eutectic-treated enzyme (blue) throughout the simulation period.*

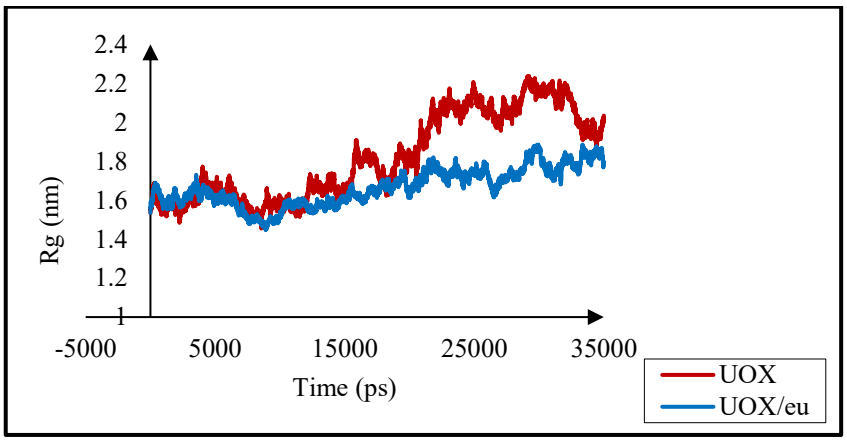

Fig 9. *Rg Analysis and its reduction in the presence (blue) of the solvent compared to the free enzyme (red).*

*Despite the fact that the glycerol concentration utilized in the current eutectic composition was twice that of the other components, it was anticipated that the interaction intensity for this formulation in the solvent would surpass that of the others. Contrary to this expectation, the results obtained from the Radial Distribution Function (RDF) analysis indicate an increase in interaction intensity in the following order: sucrose, fructose, and glycerol (***Fig *10***). This finding may be attributed to the larger molecular structure of sucrose, which possesses a greater number of hydroxyl groups compared to the other two compounds. Moreover, the most significant interactions were observed at a distance of approximately 1.5 nanometers.*

*The total energy, representing the cumulative contributions of van der Waals and electrostatic interactions, was found to be highest for sucrose, followed by fructose and glycerol (***Fig *11***). The previously mentioned structural characteristics of sucrose likely contribute to this observation, as it also exhibited the highest number of contacts among the components.*

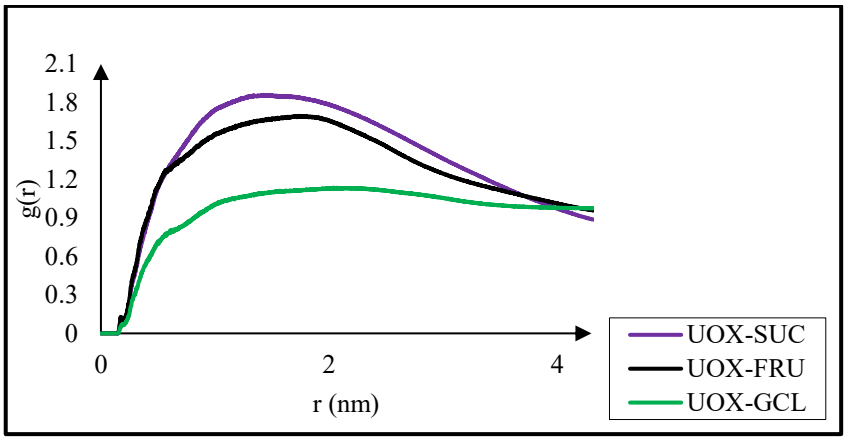

Fig 10. *RDF Analysis and assessment of interaction intensities among the constituents of the eutectic. The highest interaction intensities were recorded for sucrose (purple), followed by fructose (black) and glycerol (green).*

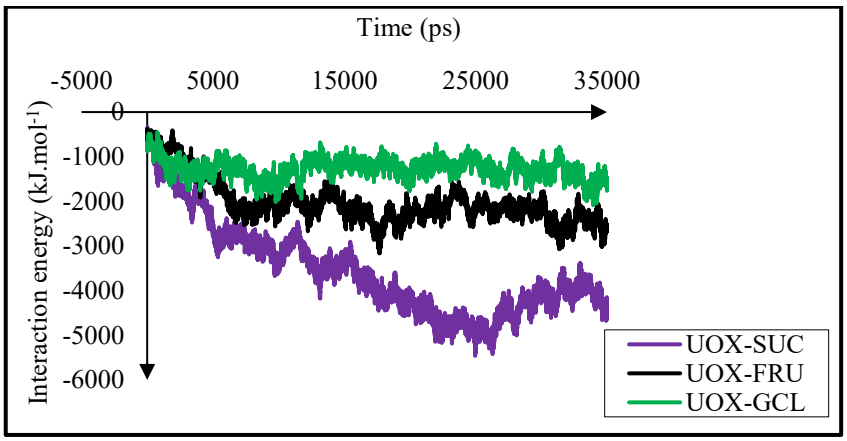

Fig 11. *Total energy calculation (comprising the sum of electrostatic and Lennard-Jones energies) for each component within the eutectic system.*

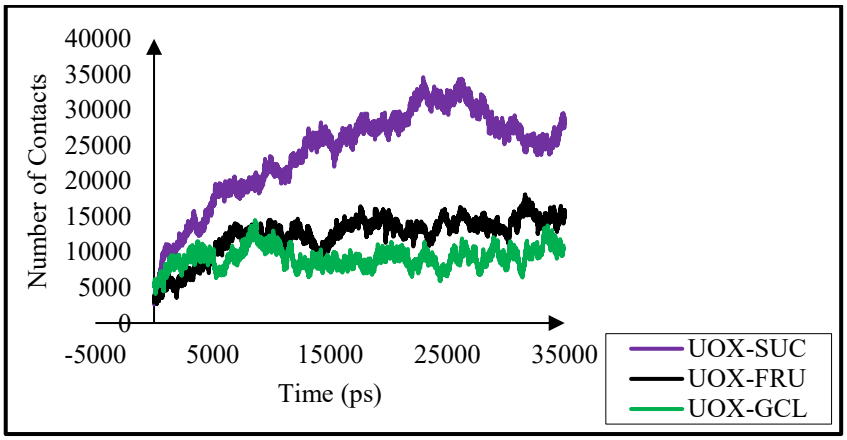

Fig 12. *Number of contacts calculation for the eutectic constituents, with sucrose depicted in purple, fructose in black, and glycerol in green.*

4. *CONCLUSION*

The role of uricase in the treatment of conditions such as gout and hyperuricemia, alongside its stability limitations due to factors like temperature, has led to a concerted effort among researchers to enhance its stability through various methodologies. In the present study, we focused on investigating the effect of a deep eutectic solvent (DES) composed of sucrose, fructose, and glycerol on the stability of uricase, employing molecular dynamics simulations. Following the cultivation of bacteria containing the uricase gene, we successfully expressed and purified the protein, ultimately synthesizing the eutectic. An optimal concentration of 5% was determined for the study. The molecular dynamics simulations conducted using specialized software, along with the corresponding analyses, revealed a notable reduction in the RMSD and an increase in structural compactness in the presence of the eutectic compared to its absence. Additionally, the observed decrease in RMSF values indicated reduced fluctuations, while the decline in SASA suggested a lower solvent-accessible surface area for the treated enzyme relative to the free enzyme, both of which are indicative of enhanced structural stability and resilience of the enzyme in this formulation. The reduction in the Radius of Gyration (Rg) further substantiated the increase in structural density. A meticulous analysis of the individual components of the eutectic revealed a significantly higher interaction intensity for sucrose relative to the other two compounds, which can be attributed to the greater number of hydroxyl groups present in this relatively larger molecule.

ACKNOWLEDEMENTS

We would like to thank the Kerman Graduate University of Advanced Technology for the support of this work.

REFERENCES

[1] *L. Gabison, N. Colloc'h, and T. Prangé, "Azide inhibition of urate oxidase," (in eng), Acta Crystallogr F Struct Biol Commun, vol. 70, no. Pt 7, pp. 896-902, Jul 2014, doi: 10.1107/s2053230x14011753.*

[2] *L. Gabison, T. Prangé, N. Colloc'h, M. El Hajji, B. Castro, and M. Chiadmi, "Structural analysis of urate oxidase in complex with its natural substrate inhibited by cyanide: Mechanistic implications," BMC Structural Biology, vol. 8, no. 1, p. 32, 2008/07/20 2008, doi: 10.1186/1472-6807-8-32.*

[3] *E. Girard et al., "Structure-function perturbation and dissociation of tetrameric urate oxidase by high hydrostatic pressure," (in eng), Biophys J, vol. 98, no. 10, pp. 2365-73, May 19 2010, doi: 10.1016/j.bpj.2010.01.058.*

[4] *B. Álvarez-Lario and J. Macarrón-Vicente, "Uric acid and evolution," (in eng), Rheumatology (Oxford), vol. 49, no. 11, pp. 2010-5, Nov 2010, doi: 10.1093/rheumatology/keq204.*

[5] *F. Dabbagh, M. B. Ghoshoon, S. Hemmati, M. Zamani, M. Mohkam, and Y. Ghasemi, "Engineering Human Urate Oxidase: Towards Reactivating It as an Important Therapeutic Enzyme," (in eng), Curr Pharm Biotechnol, vol. 17, no. 2, pp. 141-6, 2015, doi: 10.2174/1389201016666150907113055.*

[6] *G. Alvaro, R. Fernandez-Lafuente, R. M. Blanco, and J. M. Guisán, "Immobilization-stabilization of Penicillin G acylase fromEscherichia coli," Applied Biochemistry and Biotechnology, vol. 26, no. 2, pp. 181-195, 1990/11/01 1990, doi: 10.1007/BF02921533.*

[7] *S. Fetzner and R. A. Steiner, "Cofactor-independent oxidases and oxygenases," (in eng), Appl Microbiol Biotechnol, vol. 86, no. 3, pp. 791-804, Apr 2010, doi: 10.1007/s00253-010-2455-0.*

[8] *P. Retailleau et al., "Complexed and ligand-free high-resolution structures of urate oxidase (Uox) from Aspergillus flavus: A reassignment of the active-site binding mode," Acta crystallographica. Section D, Biological crystallography, vol. 60, pp. 453-62, 04/01 2004, doi: 10.1107/S0907444903029718.*

[9] *J. Maiuolo, F. Oppedisano, S. Gratteri, C. Muscoli, and V. Mollace, "Regulation of uric acid metabolism and excretion," (in eng), Int J Cardiol, vol. 213, pp. 8-14, Jun 15 2016, doi: 10.1016/j.ijcard.2015.08.109.*

[10] *H. A. Sathish, P. R. Kumar, and V. Prakash, "Mechanism of solvent induced thermal stabilization of papain," (in eng), Int J Biol Macromol, vol. 41, no. 4, pp. 383-90, Oct 1 2007, doi: 10.1016/j.ijbiomac.2007.05.009.*

[11] V. Vagenende, M. G. Yap, and B. L. Trout, "Mechanisms of protein stabilization and prevention of protein aggregation by glycerol," (in eng), Biochemistry, vol. 48, no. 46, pp. 11084-96, Nov 24 2009, doi: 10.1021/bi900649t.

[12] G. Artioli, N. Masciocchi, and E. Galli, "The Elusive Crystal Structure of Uric Acid Dihydrate: Implication for Epitaxial Growth During Biomineralization," Acta Crystallographica Section B-structural Science - ACTA CRYSTALLOGR B-STRUCT SCI, vol. 53, pp. 498-503, 06/01 1997, doi: 10.1107/S0108768196013067.

[13] M. Kutzing and B. Firestein, "Altered Uric Acid Levels and Disease States," The Journal of pharmacology and experimental therapeutics, vol. 324, pp. 1-7, 02/01 2008, doi: 10.1124/jpet.107.129031.

[14] I. R. Lee et al., "Characterization of the complete uric acid degradation pathway in the fungal pathogen Cryptococcus neoformans," (in eng), PLoS One, vol. 8, no. 5, p. e64292, 2013, doi: 10.1371/journal.pone.0064292.

[15] Q. Q. Koh et al., "Sugar-based natural deep eutectic solvent (NADES): Physicochemical properties, antimicrobial activity, toxicity, biodegradability and potential use as green extraction media for phytonutrients," Sustainable Chemistry and Pharmacy, vol. 35, p. 101218, 2023/10/01/ 2023, doi: https://doi.org/10.1016/j.scp.2023.101218.

[16] A. P. Abbott, G. Capper, D. L. Davies, R. K. Rasheed, and V. Tambyrajah, "Novel solvent properties of choline chloride/urea mixtures," Chemical communications, no. 1, pp. 70-71, 2003.

[17] L. A. Rodrigues et al., "Terpene-based natural deep eutectic systems as efficient solvents to recover astaxanthin from brown crab shell residues," ACS sustainable chemistry & engineering, vol. 8, no. 5, pp. 2246-2259, 2020.

[18] N. Gürsoy, B. Sırtbaşı, S. Şimşek, A. Elik, and N. Altunay, "Optimization and application of ultrasound-assisted sugar based deep eutectic solvent dispersive liquid–liquid microextraction for the determination and extraction of aflatoxin M1 in milk samples," Microchemical Journal, vol. 172, p. 106974, 2022/01/01/ 2022, doi: https://doi.org/10.1016/j.microc.2021.106974.

[19] S. Sinha, B. Tam, and S. M. Wang, "Applications of Molecular Dynamics Simulation in Protein Study," (in eng), Membranes (Basel), vol. 12, no. 9, Aug 29 2022, doi: 10.3390/membranes12090844.

[20] J. J. Galano-Frutos, F. Nerín-Fonz, and J. Sancho, "Calculation of Protein Folding Thermodynamics Using Molecular Dynamics Simulations," Journal of Chemical Information and Modeling, vol. 63, no. 24, pp. 7791-7806, 2023/12/25 2023, doi: 10.1021/acs.jcim.3c01107.

[21] H. Bahrami and M. Zahedi, "Comparison of the effects of sucrose molecules on alcohol dehydrogenase folding with those of sorbitol molecules on alcohol dehydrogenase folding using molecular dynamics simulation," Journal of the Iranian Chemical Society, vol. 12, 06/16 2015, doi: 10.1007/s13738-015-0671-3.

[22] A. Hospital, J. R. Goñi, M. Orozco, and J. L. Gelpí, "Molecular dynamics simulations: advances and applications," (in eng), Adv Appl Bioinform Chem, vol. 8, pp. 37-47, 2015, doi: 10.2147/aabc.S70333.

[23] D. Aioanei et al., "Single-Molecule-Level Evidence for the Osmophobic Effect Angewandte Chemie Int," Angewandte Chemie (International ed. in English), vol. 50, pp. 4394-7, 05/02 2011, doi: 10.1002/anie.201006714.

[24] D. L. Ensign, P. M. Kasson, and V. S. Pande, "Heterogeneity even at the speed limit of folding: large-scale molecular dynamics study of a fast-folding variant of the villin headpiece," (in eng), J Mol Biol, vol. 374, no. 3, pp. 806-16, Nov 30 2007, doi: 10.1016/j.jmb.2007.09.069.

[25] P. Shahmoradipour, M. Zaboli, and M. Torkzadeh-Mahani, "Exploring the impact of taurine on the biochemical properties of urate oxidase: response surface methodology and molecular dynamics simulation," Journal of Biological Engineering, vol. 18, no. 1, p. 10, 2024/01/22 2024, doi: 10.1186/s13036-023-00397-x.

[26] M. Torkzadeh-Mahani, M. Zaboli, M. Barani, and M. Torkzadeh-Mahani, "A combined theoretical and experimental study to improve the thermal stability of recombinant D-lactate dehydrogenase immobilized on a novel superparamagnetic Fe3O4 NPs@metal–organic framework," Applied Organometallic Chemistry, 03/02 2020, doi: 10.1002/aoc.5581.

[27] H. Berendsen, J. P. M. Postma, W. van Gunsteren, A. D. DiNola, and J. R. Haak, "Molecular-Dynamics with Coupling to An External Bath," The Journal of Chemical Physics, vol. 81, p. 3684, 10/15 1984, doi: 10.1063/1.448118.

[28] G. Bussi, D. Donadio, and M. Parrinello, "Canonical sampling through velocity rescaling," (in eng), J Chem Phys, vol. 126, no. 1, p. 014101, Jan 7 2007, doi: 10.1063/1.2408420.

[29] A. C. Simmonett and B. R. Brooks, "A compression strategy for particle mesh Ewald theory," (in eng), J Chem Phys, vol. 154, no. 5, p. 054112, Feb 7 2021, doi: 10.1063/5.0040966.

[30] J. Feher, "1.4 - Chemical Foundations of Physiology I: Chemical Energy and Intermolecular Forces," in Quantitative Human Physiology (Second Edition), J. Feher Ed. Boston: Academic Press, 2017, pp. 46-58.

[31] B. Hess, H. Bekker, H. Berendsen, and J. Fraaije, "LINCS: A Linear Constraint Solver for molecular simulations," Journal of Computational Chemistry, vol. 18, 04/30 1998, doi: 10.1002/(SICI)1096-987X(199709)18:123.0.CO;2-H.

[32] J. Monroe and M. Shirts, "Converging free energies of binding in cucurbit[7]uril and octa-acid host–guest systems from SAMPL4 using expanded ensemble simulations," Journal of computer-aided molecular design, vol. 28, 03/08 2014, doi: 10.1007/s10822-014-9716-4.

[33] X. Gao, Z. Liu, W. Cui, L. Zhou, Y. Tian, and Z. Zhou, "Enhanced thermal stability and hydrolytic ability of Bacillus subtilis aminopeptidase by removing the thermal sensitive domain in the non-catalytic region," (in eng), PLoS One, vol. 9, no. 3, p. e92357, 2014, doi: 10.1371/journal.pone.0092357.

[34] J. Wang, R. Saxena, S. K. Vanga, and V. Raghavan, "Effects of Microwaves, Ultrasonication, and Thermosonication on the Secondary Structure and Digestibility of Bovine Milk Protein," Foods, vol. 11, p. 138, 01/06 2022, doi: 10.3390/foods11020138.

[35] Y. Lee et al., "Dissecting the critical factors for thermodynamic stability of modular proteins using molecular modeling approach," (in eng), PLoS One, vol. 9, no. 5, p. e98243, 2014, doi: 10.1371/journal.pone.0098243.

[36] [Online]. Available: https://www.eurofins.in/genomics/blog/advantage-of-expression-cloning-in-pet28a-plus-vector/.

[37] A. Teimoori, H. Soleimanjahi, F. Fotouhi, and Z. Meshkat, "Isolation and cloning of human papillomavirus 16 L1 gene from Iranian isolate," Saudi medical journal, vol. 29, pp. 1105-8, 09/01 2008.

[38] L. Cai, Q. Li, Y. Deng, X. Liu, W. Du, and X. Jiang, "Construction and expression of recombinant uricase-expressing genetically engineered bacteria and its application in rat model of hyperuricemia," (in eng), Int J Mol Med, vol. 45, no. 5, pp. 1488-1500, May 2020, doi: 10.3892/ijmm.2020.4512.

[39] J. Li et al., "High-level expression, purification, and characterization of non-tagged Aspergillus flavus urate oxidase in Escherichia coli," (in eng), Protein Expr Purif, vol. 49, no. 1, pp. 55-9, Sep 2006, doi: 10.1016/j.pep.2006.02.003.

[40] M. Pazhang, K. Khajeh, and B. Ranjbar, "Effects of water-miscible solvents and polyhydroxy compounds on the structure and enzymatic activity of TLN," Journal of biotechnology, vol. 127, pp. 45-53, 01/01 2007, doi: 10.1016/j.jbiotec.2006.05.017.

[41] T.-Y. Lin and S. N. Timasheff, "Why do some organisms use a urea-methylamine mixture as osmolyte? Thermodynamic compensation of urea and trimethylamine N-oxide interactions with protein," Biochemistry, vol. 33, no. 42, pp. 12695-12701, 1994/10/01 1994, doi: 10.1021/bi00208a021.

[42] M. Zaboli, F. Saeidnia, M. Zaboli, and M. Torkzadeh-Mahani, "Stabilization of recombinant d-Lactate dehydrogenase enzyme with trehalose: Response surface methodology and molecular dynamics simulation study," Process Biochemistry, vol. 101, pp. 26-35, 2021/02/01/ 2021, doi: https://doi.org/10.1016/j.procbio.2020.11.001.

[43] S. Ghanbari-Ardestani et al., "The effect of different percentages of triethanolammonium butyrate ionic liquid on the structure and activity of urate oxidase: Molecular docking, molecular dynamics simulation, and experimental study," Journal of Molecular Liquids, vol. 292, p. 111318, 2019/10/15/ 2019, doi: https://doi.org/10.1016/j.molliq.2019.111318.